frequency of which is in the gigahertz region.

Acknowledgment. We thank Dr. K. Nagayama for helpful discussions. This work was partly supported by a Grant-in-Aid for Scientific Research from the Ministry of Education, Japan.

References and Notes

(1) This work was performed at the Department of Physics, Faculty of Science, University of Tokyo, Tokyo, Japan.
(2) Wada, A. *Adv. Biophys.* **1976**, *9*, 1–63.
(3) Grant, E. H.; Sheppard, R. J.; South, G. P. "Dielectric Behaviour of Biological Molecules in Solution"; Clarendon Press: Oxford, 1978.
(4) Husimi, Y.; Wada, A. *Rev. Sci. Instrum.* **1976**, *47*, 213.
(5) Nakamura, H.; Husimi, Y.; Wada, A. *J. Appl. Phys.* **1981**, *52*, 3053.
(6) Cole, R. H.; Mashimo, S.; Winsor, P., IV. *J. Phys. Chem.* **1980**, *84*, 786.
(7) McCammon, J. A.; Gelin, B. R.; Karplus, M. *Nature (London)* **1977**, *267*, 585.
(8) Wagner, G.; Wüthrich, K. *Nature (London)* **1978**, *275*, 247.
(9) Frauenfelder, H.; Petsko, G. A.; Tsernoglou, D. *Nature (London)* **1979**, *280*, 558.
(10) Artymiuk, P. J.; Blake, C. C. F.; Grace, D. E. P.; Oatley, S. J.; Phillips, D. C.; Sternberg, M. J. E. *Nature (London)* **1979**, *280*, 563.
(11) Patel, D. J.; Canuel, L. L. *Proc. Natl. Acad. Sci. U.S.A.* **1976**, *73*, 1398.
(12) Nagayama, K.; Okada, S. *Polym. J.* **1973**, *5*, 97.
(13) Fröhlich, H. "Theory of Dielectrics"; Clarendon Press: Oxford, 1958.
(14) Nakamura, H.; Husimi, Y.; Parry-Jones, G.; Wada, A. *J. Chem. Soc., Faraday Trans. 2* **1977**, *73*, 1178.
(15) Itoh, K.; Shimanouchi, T. *Biopolymers* **1970**, *9*, 383.
(16) Davies, M. *J. Chem. Educ.* **1969**, *46*, 17.
(17) Allerhand, A.; Oldfield, E. *Biochemistry* **1973**, *12*, 3428.
(18) Nagayama, K. *Biophysics* (in Japanese) **1976**, *16*, 68.
(19) Kinoshita, K., Jr.; Kawato, S.; Ikegami, A. *Biophys. J.* **1977**, *20*, 289.

Chain Characteristics and Counterion Binding of Poly(*N*-vinylimidazole) and Its Protonated and Quaternized Salts

J. S. Tan* and A. R. Sochor

Research Laboratories, Eastman Kodak Company, Rochester, New York 14650.

Received March 5, 1981

ABSTRACT: Intrinsic viscosity, light scattering, and turbidimetric titration were used to characterize the solution behavior of poly(*N*-vinylimidazole) and its charged polycations, including the protonated and the quaternized forms. The unperturbed dimensions of these chain molecules are not sensitive to the solvents or the side groups at the quaternary ammonium site but are sensitive to the counterions. The characteristic ratio C_∞ is 15–18 for polymers with the stronger binding chloride ion as the counterion but increases to 28 when the counterion is replaced by the weaker binding acetate or propionate ion. The order of counterion binding is similar to the order for the Hofmeister series. The persistence lengths estimated according to the scheme of Yamakawa and Fujii based on the wormlike-chain model are 22–23 Å for neutral poly(*N*-vinylimidazole) and 20 Å for the quaternized salt.

Poly(*N*-vinylimidazole) (PVI) and its quaternary ammonium salt poly(3-benzyl-1-vinylimidazolium chloride) (QPVI) can be considered as model polymers for investigating the interactions of similar polymers with neutral salts, complexing metal ions, and dye molecules. Substantial work has been reported concerning viscometric, potentiometric, and conductometric behavior of PVI and its quaternary salts in aqueous media,[1-3] the catalytic effect of imidazole-containing polymers,[4] and complex formation of PVI with metal ions.[5] Little effort has been made to investigate chain flexibility of these polymers as affected by the nature of the solvents, the type of neutral electrolytes present, or the structure of the side group at the quaternized site.

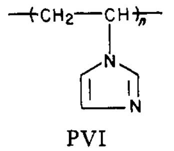

PVI

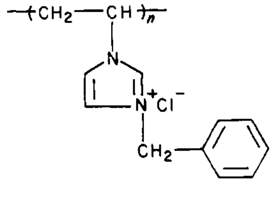

QPVI

We report here the solubility behavior of PVI, QPVI, and the protonated polymer HPVI. The unperturbed dimensions of these polymers were determined by light scattering and intrinsic viscosity. These results are related to counterion binding data obtained by turbidimetric titration. The effect of counterion binding on dye binding will also be discussed. The conformational change of PVI upon protonation, as studied by potentiometry, viscometry, and ^{1}H NMR was reported elsewhere.[6]

Experimental Section

Materials. PVI was synthesized by polymerization of *N*-vinylimidazole (BASF Chemicals) with azobis(isobutyronitrile) as the catalyst. Distilled monomer (150 g) was dissolved in 980 mL of benzene and polymerized at 60 °C under a nitrogen atmosphere for 48 h with 1.3 g of catalyst. The polymer was precipitated as a white powder. The solid was collected by filtration and was oven-dried at 35 °C. Two batches of the whole polymer were used for further fractionation in this study. Previous NMR studies suggested that this polymer is atactic.[6]

PVI was fractionated by stepwise precipitation with two solvent–nonsolvent pairs: *n*-butyl alcohol + *n*-hexane (for polymer batch I) and methanol + toluene (for polymer batch II). The coacervate liquids were freeze-dried, and the solids were heated at 40 °C under vacuum in the presence of P_2O_5 for several weeks before use. The weight-average molecular weights, $\bar{M}_w$, of the fractions, as determined by light scattering in methanol, ranged from 1.3×10^6 to 5.5×10^4.

Portions of several of the PVI fractions in batch I were then converted into the quaternized form. An excess of benzyl chloride was added to each PVI fraction dissolved in dimethylformamide. The mixture was heated at 85 °C on a steam bath for 3 h to allow complete quaternization. The quaternized polymer was precipitated by addition of acetone. The solids were puified by redissolving them in methanol and precipitating them with acetone. These steps were repeated once again before the polymer was dried

0024-9297/81/2214-1700$01.25/0

Table I
Intrinsic Viscosity and Light Scattering Data for PVI in MeOH/TBABr[a]

fraction	$[\eta]$, dL/g	$\bar{M}_w \times 10^{-3}$	$\langle s_z^2 \rangle^{1/2}$, Å	$A_2 \times 10^4$, mol·mL/g	α_η
batch I					
I_2	2.34	590	460	5.2	1.21
I_3	1.86	340	350	7.5	1.23
I_4	1.63	280	300	7.7	1.22
I_5	1.02	150	200	13.0	1.16
I_6	0.51	55	130	20.0	1.08
A	2.20	500			1.22
batch II					
II_1	3.58	1300	800	3.2	1.23
II_2	2.58	900	620	4.0	1.17
II_3	1.90	500	390	6.2	1.16
II_4	1.37	270	300	10.0	1.16
II_5	1.15	195	250	12.0	1.15
II_6	0.67	93	200	16.0	1.08

[a] Batch I, 0.001 M; batch II, 0.01 M.

at 35 °C. The quaternized fractions were then dialyzed against distilled water and freeze-dried at 40 °C under vacuum for 2 weeks before use. Elemental analyses for nitrogen and chlorine indicated that these samples were fully quaternized.

The protonated form of PVI (HPVI) was obtained by neutralizing PVI with a molar equivalent of an acid such as hydrochloric, acetic, or propionic acid.

Methods. Light Scattering and Intrinsic Viscosity. These data were obtained at 25 °C by using a Sofica photometer with unpolarized light at 436 nm and the Ubbelohde microviscometers. Details of the experimental procedures and data treatments were reported previously for other polymers.[7] The samples in aqueous salt solutions were dialyzed for 24 h before measurements. The difference in the refractive index increment, dn/dc, for the dialyzed and undialyzed solutions in methanol/tetrabutylammonium bromide (TBABr) was negligible. Therefore, the undialyzed solutions were used for light scattering measurements in this organic medium. This procedure was appropriate because the molecular weight of a given polymer measured in dialyzed aqueous salt solution was similar to that measured in undialyzed organic solution. The refractive index increment for PVI in methanol was 0.235, which compares well with the value (0.227) obtained by Tricot et al.[8] A value of 0.224 was measured for QPVI in methanol. Experimental uncertainties were estimated to be as follows: dn/dc, ±2%; $\bar{M}_w$, ±5%; second virial coefficient A_2, ±10%; radius of gyration $\langle s_z^2 \rangle^{1/2}$, ±10%; intrinsic viscosity $[\eta]$, ±2%.

Turbidimetric Titration. Concentrated salt solutions were used to titrate 3 mL of a 1% polymer solution stirred with a magnetic bar. The onset of turbidity was observed by the scattering of incident light from a microscope lamp. The concentration of the salt in the polymer solution at the cloud point was calculated and used as a relative measure of counterion binding.

Results

Water and several alcohols (methyl, ethyl, isopropyl, n-butyl, and isobutyl) were good solvents for PVI and QPVI. A concave-upward curvature was observed in the viscosity plots (i.e., η_{sp}/C_p vs. C_p or ln η_{rel}/C_p vs. C_p, where η_{sp} and η_{rel} are the specific and relative viscosities, respectively, and C_p is the polymer concentration in g/dL) for the above solutions, indicating the effect of the ionization of polymer upon dilution. Linear viscosity plots were obtained, however, when neutral salts, such as TBABr or sodium chloride, were added.

The intrinsic viscosity data for a fraction of PVI (I_5, $\bar{M}_w$ = 1.5 × 10^5) in methanol/H_2O (v/v)/0.001 M TBABr as a function of solvent composition are presented in Figure 1.

Light scattering and intrinsic viscosity data in methanol/TBABr are listed in Table I for PVI and in Table II for QPVI. The intrinsic viscosity–molecular weight relationships in methanol/TBABr and in several aqueous salt solutions are presented as double-logarithmic plots of $[\eta]$ vs. $\bar{M}_w$ according to the Mark–Houwink expression

$$[\eta] = KM^{\nu} \quad (1)$$

where K and ν are empirical parameters. These results are

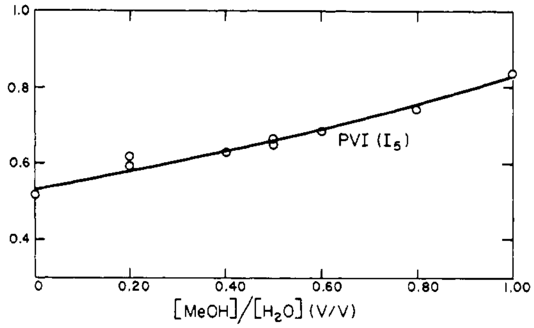

Figure 1. Intrinsic viscosity vs. [MeOH]/[H_2O] (v/v) for PVI (I_5, $\bar{M}_w$ = 1.5 × 10^5) in methanol/H_2O/0.001 M TBABr.

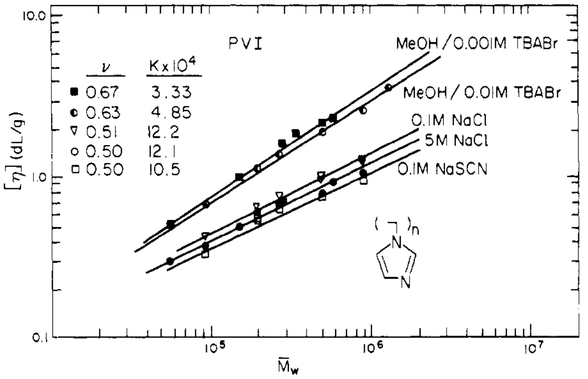

Figure 2. Mark–Houwink plots, $[\eta] = K\bar{M}_w^{\nu}$, for PVI in methanol/TBABr and in aqueous salt solutions.

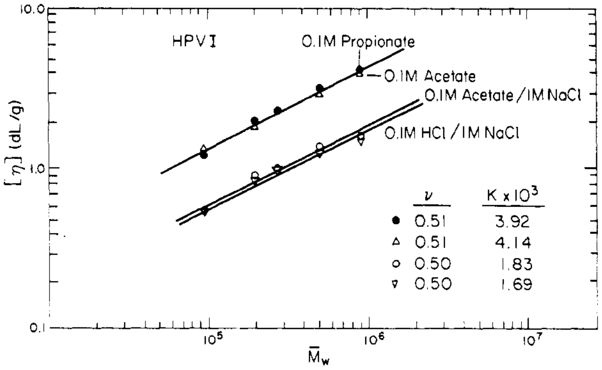

Figure 3. Mark–Houwink plots, $[\eta] = K\bar{M}_w^{\nu}$, for HPVI in aqueous salt solutions.

Table II
Intrinsic Viscosity and Light Scattering Data for QPVI in MeOH/0.01 M TBABr

fraction	$[\eta]$, dL/g	$\bar{M}_w \times 10^{-3}$	$\langle s_z^2 \rangle^{1/2}$, Å	$A_2 \times 10^4$, mol·mL/g	α_η
QI_2	1.07	1600	560	2.0	1.12
QI_3	0.95	1300	460	2.6	1.11
QI_4	0.80	930	360	3.2	1.11
QI_5	0.54	470	250	6.0	1.09
QI_6	0.27	180	120	9.3	1.02

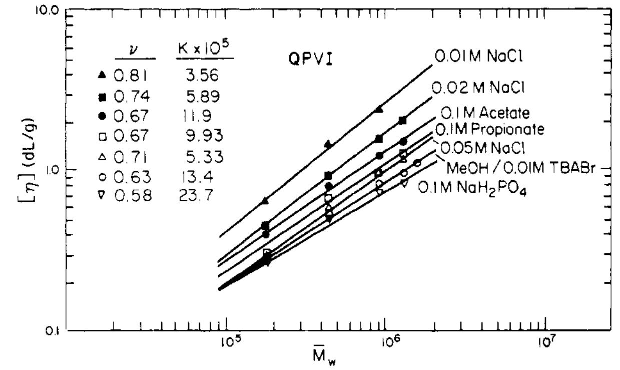

Figure 4. Mark–Houwink plots, $[\eta] = K\bar{M}_w^{\nu}$, for QPVI in methanol/0.01 M TBABr and in aqueous salt solutions.

Table III
Turbidimetric Titration Data

Na salt	[Na salt], M, in solutions of PVI	HPVI	QPVI
acetate	–[a]	–	1.12
propionate			0.78
butyrate			0.56
formate			0.50
sulfate			0.35
phosphate (monobasic)			0.32
chloride	–	–	0.096
tartrate			0.027
ethyl sulfate			0.017
bromide	–	–	0.006
iodide	–	0.962	0.0016
perchlorate	–	0.059	0.0012
thiocyanate	–	0.264	0.00083

[a] "–" indicates that no precipitate was observed in the saturated salt solution.

shown in Figure 2 for PVI in methanol/TBABr, aqueous NaCl, and NaSCN solutions, in Figure 3 for HPVI in aqueous acetate, propionate, and NaCl solutions, and in Figure 4 for QPVI in methanol/TBABr and several aqueous salt solutions.

The concentrations of sodium salts required to cause turbidity of the polymer solutions are listed in Table III.

Discussion

Effects of Solvent and Neutral Salts on Solubility. Our intrinsic viscosity measurements for PVI and QPVI indicate that the presence of a supporting electrolyte is necessary to obtain a linear plot for [η]. The presence of the polyelectrolyte effect was not discussed by other workers in two publications[8,9] concerning viscosity studies of poly(*N*-vinylimidazole) in alcohols, and hence their [η] data are somewhat questionable.

1. Water Is an Ideal Solvent for PVI. Figure 1 shows that methanol is a better solvent than water for PVI. The fact that this hydrophobic chain is soluble in water suggests that the affinity of this polymer for water may be caused by the formation of hydrogen bonds between the imidazole and water molecules. As shown in Figure 2, the Mark–Houwink exponent for PVI is ~0.5 in aqueous salt solutions and is independent of ionic strength. This suggests that water is an ideal (or Θ) solvent and that added electrolytes do not alter chain conformation. In fact, the highest fraction of PVI (II_1, $\bar{M}_w = 1.3 \times 10^6$) did not dissolve completely in aqueous media.

The light scattering data also showed that water is a Θ solvent for PVI. The second virial coefficients for fraction II_5 of PVI in aqueous NaCl solutions (0.01, 0.1, 1, and 5 M) were measured to be less than 1×10^{-4} (mol·mL/g).

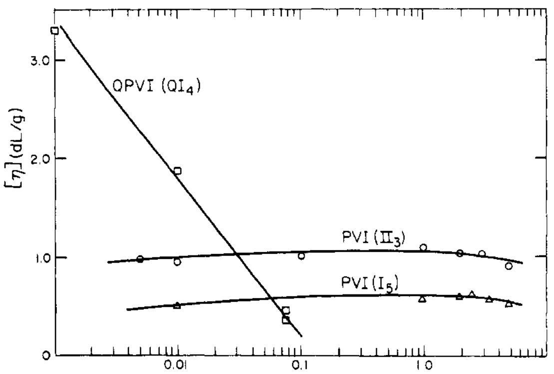

Figure 5. Intrinsic viscosity vs. log [NaCl] for QPVI (QI_4, $\bar{M}_w = 9.3 \times 10^5$), PVI ($II_3$, $\bar{M}_w = 5.0 \times 10^5$), and PVI ($I_5$, $\bar{M}_w = 1.5 \times 10^5$) in aqueous NaCl solutions.

To further examine the nature of the interaction between PVI and water, we added several hydrogen-bond breakers to the aqueous polymer solution. A phase separation was indeed observed when enough trifluoroacetic acid was added. This phenomenon of phase separation caused by trifluoroacetic acid (a strong hydrogen-bond breaker for solute–solvent interaction or a strong hydrogen-bonding agent) and the slight effect of neutral salts on solubility and viscosity of the polymer strongly suggest the formation of hydrogen bonds between the imidazole groups and water.

2. Effect of Ionic Strength on [η] for PVI and QPVI. Although neutral salts have little effect on the intrinsic viscosity and chain dimensions of the uncharged polymer PVI, as discussed above (Figure 2), they have a strong influence on the charged polymer QPVI. These results are shown in Figure 5 for comparison, where the intrinsic viscosities are plotted against log (ionic strength, C_{NaCl}) for QPVI (fraction QI_4) and PVI (fractions II_3 and I_5). The intrinsic viscosities for the two PVI fractions (II_3, I_5) are virtually unchanged with ionic strength. The intrinsic viscosity for the quaternized fraction (QI_4), on the other hand, decreases linearly with log (ionic strength).

The effect of ionic strength on chain dimensions can also be demonstrated by the decrease in the Mark–Houwink exponent, ν, with increasing ionic strength, as shown in Figure 4 for QPVI in aqueous salt media. These results are typical of the behavior of polyions whose chain dimensions vary greatly with the concentration and binding strength of the counterion in solution.

3. Acidic Solutions Are Ideal Solvents for PVI. The Mark–Houwink plots and the values for the slopes, as shown in Figure 3 for the fully neutralized polymer HPVI, indicate that acidic aqueous salt solutions are ideal (or Θ) solvents for PVI, although the unperturbed dimensions of HPVI may vary with the counterion present. This result is correlated with the extent of counterion binding (discussed later).

4. Effect of Added Salts on Turbidity of PVI and QPVI Solutions. The amount of neutral salt required to precipitate a charged polyion depends on the effectiveness of counterion binding or charge screening by the added salts. Hence, turbidimetric titration data can be used as relative measures of the strength of counterion binding to polymers. For the water-soluble, uncharged PVI, no turbidity was observed upon addition of the salts listed in Table III. This implies that neutral electrolytes are ineffective in altering the interaction between the imidazole group and the water molecules which is presumably hydrogen bonding. This result is consistent with the viscosity measurements for PVI in aqueous salt solutions,

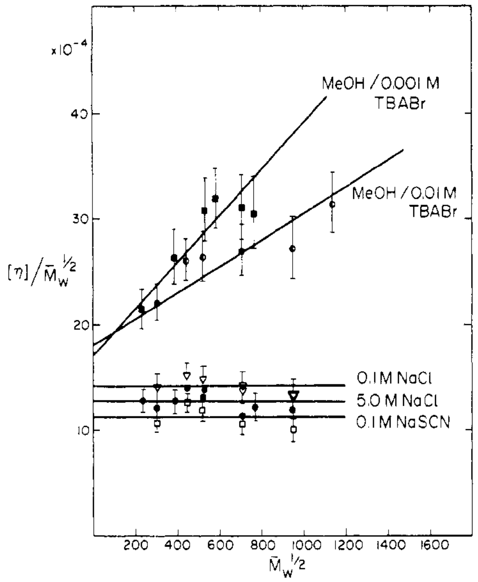

Figure 6. $[\eta]/\bar{M}_w^{1/2}$ vs. $\bar{M}_w^{1/2}$ for PVI in methanol and aqueous salt solutions.

in which the intrinsic viscosity is insensitive to ionic strength.

For the charged polycations HPVI and QPVI, the stability of the polymer solution is sensitive to the presence and concentration of neutral electrolytes. For HCl-neutralized HPVI, only I^-, ClO_4^-, and SCN^- cause turbidity. For benzyl chloride quaternized QPVI, the neutral salts are even more effective as precipitants, probably because of the hydrophobic nature of the side groups of the polymer. The order of increasing precipitating power by the sodium salts from acetate to SCN^- (Table III) is consistent with that for the Hofmeister series found for proteins.[10] The more effective precipitants of the SCN^- end of the series are highly polarized and bind strongly to the quaternized sites, whereas the less effective precipitants at the acetate end of the series are less polar and bind weakly to the polycation. The order of decreasing effectiveness of the carboxylate anions as precipitants for QPVI (formate > butyrate > propionate > acetate, Table III) does not follow the order of increasing size of the alkyl substituents, however.

The extent of counterion binding to polycations, as studied here by turbidimetric titration, will be correlated with the unperturbed dimensions of the polymers (next section).

Unperturbed Dimensions. 1. Stockmayer–Fixman Plots. Chain flexibilities of PVI, QPVI, and HPVI, as affected by the polarity of the solvent and by counterions, are discussed below in terms of the unperturbed dimensions. The larger the unperturbed dimensions, the less flexible the chain becomes. These dimensions were estimated by linear extrapolation based on the intrinsic viscosity–molecular weight data according to the Stockmayer–Fixman equation

$$[\eta]/\bar{M}_w^{1/2} = K_0 + 0.51\Phi_0 B\bar{M}_w^{1/2} \qquad (2)$$

where K_0 is the intercept for the plot of $[\eta]/\bar{M}_w^{1/2}$ vs. $\bar{M}_w^{1/2}$, B is related to the second virial coefficient and is assumed to be constant for all molecular weights, and Φ_0 is the Flory universal constant (2.6×10^{21} in units of dL/g for $[\eta]$). The unperturbed end-to-end distance, $\langle r_0^2\rangle^{1/2}$, is related to K_0 by

$$\langle r_0^2\rangle = \left(\frac{K_0}{\Phi_0}\right)^{2/3}\bar{M}_w \qquad (3)$$

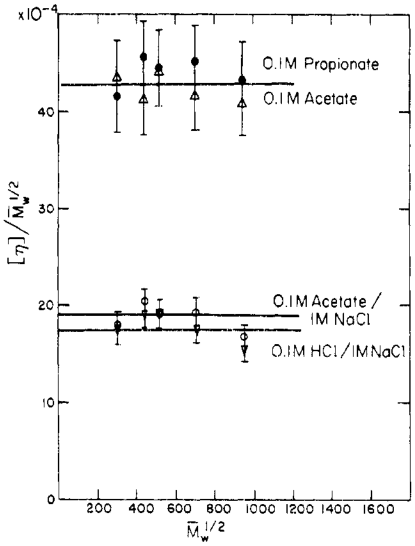

Figure 7. $[\eta]/\bar{M}_w^{1/2}$ vs. $\bar{M}_w^{1/2}$ for HPVI in aqueous salt solutions.

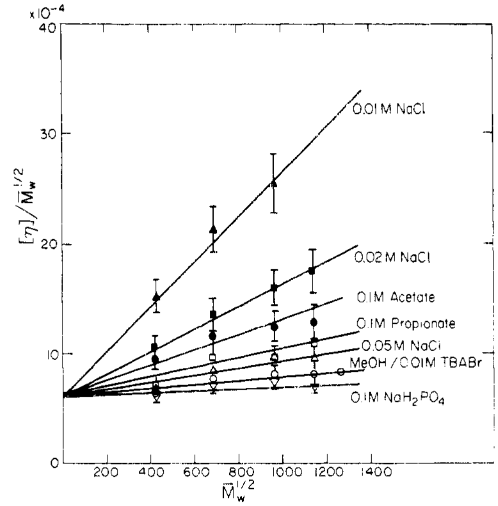

Figure 8. $[\eta]/\bar{M}_w^{1/2}$ vs. $\bar{M}_w^{1/2}$ for QPVI in methanol/0.01 M TBABr and in aqueous salt solutions.

Instead of $\langle r_0^2\rangle$, we have used the characteristic ratio defined by

$$C_\infty = \frac{\langle r_0^2\rangle}{nl^2} = \left(\frac{K_0}{\Phi_0}\right)^{2/3}\frac{M_0}{2l^2} \qquad (4)$$

as a measure of chain flexibility, where M_0 is the monomer molecular weight, n is the number of backbone bonds, and l is the corresponding bond length.

The Stockmayer–Fixman plots are shown in Figures 6–8 for PVI, HPVI, and QPVI, respectively. The data points for PVI (Figure 6) and HPVI (Figure 7) appeared to have larger scatter than those for QPVI (Figure 8). Because of the large errors involved in determining $[\eta]/\bar{M}_w^{1/2}$, the straight lines drawn through the data points were used to obtain the intercepts. The uncertainty for the intercept, K_0, when the experimental errors in $\bar{M}_w$ and $[\eta]$ were taken into account, was estimated to be ±10–15%. Considering this uncertainty, we used the average values for K_0 to calculate the corresponding values for C_∞ (Table IV).

2. Effect of Solvents, Protonation, and Quaternization on C_∞. The characteristic ratio for neutral PVI in methanol ($C_\infty = 15$) is slightly higher than the value in aqueous salt solutions ($C_\infty = 12$), indicating some effect of solvent polarity on the unperturbed dimensions. The C_∞ value for HPVI (with acetate or chloride as the coun-

Table IV
Characteristic Ratios C_∞

polymer	C_∞	medium
PVI	15 (±2)	MeOH/TBABr (0.001, 0.01 M)
	12	aq NaCl (0.1, 5 M) aq NaSCN (0.1 M)
HPVI[a]	15	aq NaCl (1 M)
HPVI[b]	16	aq NaCl (1 M)
HPVI[b]	28	aq acetate (0.1 M)
HPVI[c]	28	aq propionate (0.1 M)
QPVI	18	MeOH/TBABr (0.01 M)
	18	aq NaCl (0.01, 0.02, 0.05 M) aq NaH_2PO_4 (0.1 M) aq propionate (0.1 M)
	18	aq acetate (0.1 M)

[a] PVI was neutralized with HCl. [b] PVI was neutralized with acetic acid. [c] PVI was neutralized with propionic acid.

terion) in aqueous 1 M NaCl is 15 or 16 (Table IV), suggesting a minimum effect of protonation on $\langle r_0^2\rangle^{1/2}$ as long as excess chloride ions are present. On the contrary, a remarkably high C_∞ value (28) was measured for HPVI in the presence of acetate or propionate ions. We believe this to be a result of weaker counterion binding by the bulky and less polar acetate or propionate ions.

The characteristic ratio for QPVI is 18 in methanol and in aqueous salt solutions (Table IV), indicating no effect of solvent polarity on the unperturbed dimensions of this charged polymer. The smaller value of C_∞ (18) for $QPVI^+Cl^- + OAc^-$ than that (C_∞ = 28) for the protonated polymer ($HPVI^+OAc^- + OAc^-$) may be caused by the incomplete counterion exchange in the former system due to the stronger binding Cl^- present.

In summary, the unperturbed dimensions of the imidazole-containing vinyl polymers depend very little on the polarity of the solvent, the charge of the imidazole nitrogen, or the side-chain groups attached to the quaternary ammonium site. They vary greatly, however, with the type of counterions associated with the quaternized group. The stronger binding ions, such as chloride or those above it in the Hofmeister series, tend to collapse the polymer coil to a greater extent (smaller C_∞) than the weaker binding ions, such as acetate. This ion binding has a great effect on the binding of a negatively charged dye molecule to this positively charged polymer. When the counterion binding is the strongest, as with SCN^-, competition for the binding site of the polymer is the greatest, resulting in weak dye binding. Therefore, acetate counterion should be used to achieve stronger polymer–dye interaction.

Although the effect of counterion binding strength is reflected in the unperturbed dimensions measured, the viscosity–molecular weight relationship is not sensitive enough to distinguish the difference between the effects of the two neighboring counterions in the Hofmeister series on the unperturbed dimensions of the parent polycation. Only when the two ions are far enough apart in the series, such as acetate and chloride ions, can the C_∞ values reveal some significant difference.

Coillike Behavior. 1. Dependence of $\langle s_z^2\rangle$ on $\bar{M}_w$. The coillike behavior of these polymers was further examined by the molecular weight dependence of the radius of gyration. Using the wormlike-coil model originally proposed by Kratky and Porod,[11] Benoit and Doty[12] derived the equation

$$\langle s^2\rangle = q^2\left[\frac{x}{3} - 1 + \frac{2}{x} - \frac{2}{x^2}(1 - e^{-x})\right] \tag{5}$$

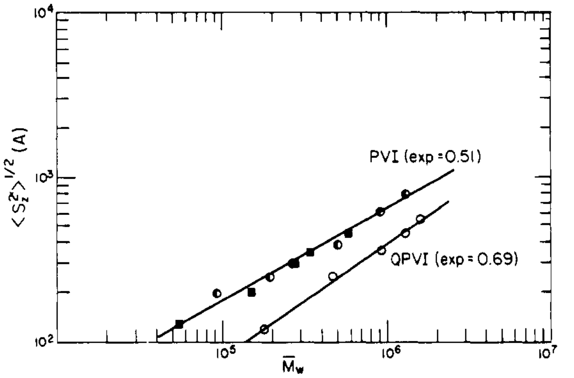

Figure 9. $\langle s_z^2\rangle^{1/2}$ vs. $\bar{M}_w$ for PVI and QPVI in methanol/TBABr.

where q is the persistence length, $x = Nb/q$, b is the monomeric projection along the contour direction, and N is the degree of polymerization. For the limiting case of coillike behavior ($x \rightarrow \infty$)

$$\lim_{x\to\infty} \frac{\langle s^2\rangle}{N} = \frac{bq}{3} \tag{6}$$

and for the other limiting case of rodlike behavior ($x \rightarrow 0$)

$$\lim_{x\to 0} \frac{\langle s^2\rangle^{1/2}}{N} = \left(\frac{b^2}{12}\right)^{1/2} \tag{7}$$

Since N is proportional to molecular weight M, and b and q are molecular parameters independent of molecular weight, we obtain from eq 6 and 7 the following relations:

$$\langle s^2\rangle^{1/2} \propto M^{0.50} \quad \text{for the coillike limit}$$

and

$$\langle s^2\rangle^{1/2} \propto M^{1.0} \quad \text{for the rodlike limit}$$

The $\langle s_z^2\rangle^{1/2}$ and $\bar{M}_w$ data for PVI and QPVI in methanol/0.01 M TBABr (good solvent according to $[\eta]$ data) are presented in double-logarithmic plots in Figure 9. The data points fall into the following linear relations:

$$\langle s_z^2\rangle^{1/2} = k_1\bar{M}_w^{0.51} \quad \text{(for PVI)}$$

and

$$\langle s_z^2\rangle^{1/2} = k_2\bar{M}_w^{0.69} \quad \text{(for QPVI)}$$

where k_1 and k_2 are parameters. The values for the exponents obtained here fall in the range for flexible coils. The higher value for QPVI than for PVI is attributed to the bulky benzyl group at the quaternized site in MeOH/0.01 M TBABr.

2. Dependence of A_2 on $\bar{M}_w$. The excluded volume u for a solid sphere with radius R is[13]

$$u = (32/3)\pi R^3 = 8Mv/N_A \tag{8}$$

where v is the specific volume, M is the molecular weight, and N_A is Avogadro's number. The second virial coefficient is expressed as[13]

$$A_2 = 16\pi N_A R^3/3M^2 = 4u/M \tag{9}$$

The corresponding equations for u and A_2 for a rigid rod with L as the cylindrical length and d as the diameter are[13]

$$u = \tfrac{1}{2}\pi dL^2 = 2LMv/dN_A \tag{10}$$

and

$$A_2 = Lv/dM \tag{11}$$

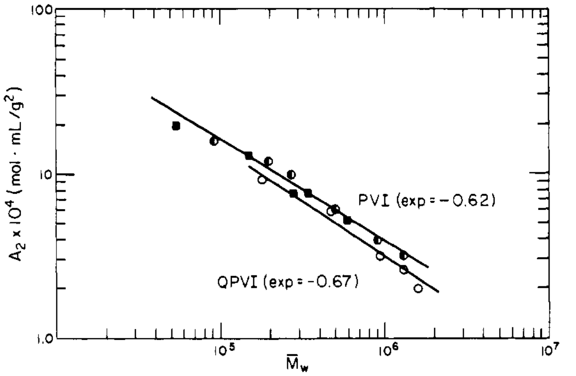

Figure 10. A_2 vs. $\bar{M}_w$ for PVI and QPVI in methanol/TBABr.

According to eq 9 and 11, A_2 would vary with $1/M$ for the solid-sphere model and would be independent of M for the rigid-rod model, where L is proportional to M.

The double-logarithmic plots of A_2 vs. $\bar{M}_w$ are shown in Figure 10 for PVI and QPVI in methanol. The data points fall into the following linear relations:

$$A_2 = m_1\bar{M}_w^{-0.62} \qquad \text{(for PVI)}$$

and

$$A_2 = m_2\bar{M}_w^{-0.67} \qquad \text{(for QPVI)}$$

where m_1 and m_2 are parameters. The absolute values for these exponents are much higher than those reported for random-coil polymers, such as polyisobutylene in cyclohexane ($A_2 \propto M^{-0.14}$) and polystyrene in toluene ($A_2 \propto M^{-0.22}$).[14,15] Nevertheless, the present values are in the middle of the range for solid-sphere and rigid-rod models.

The above light scattering results (Figures 9 and 10) show that these polymers are coillike in methanol/TBABr. This finding is consistent with the viscosity data in which the Mark–Houwink exponent calculated for these two polymers in methanol/TBABr is $\nu = 0.63$ (see data for MeOH/TBABr in Figures 2 and 4).

Application of the Wormlike-Chain Model. In the Kratky–Porod wormlike-chain model, polymers are considered to be composed of a number of segments characterized by a stiffness parameter, the "persistence length" q. When q is large, the polymer is rodlike; when q is small, the polymer is coillike. Here we have adopted the scheme of Yamakawa and Fujii[16] based on the wormlike-chain model to treat the viscosity data.

The intrinsic viscosity is expressed as

$$[\eta] = 10^{-2}\Phi L_r^{3/2}/\lambda^3 M \qquad (12)$$

where λ^{-1} is the Kuhn statistical length and is equal to $2q$; L_r is the reduced contour length or the total number of Kuhn segments and is related to the contour length or molecular weight M by

$$L_r = \lambda L = M/M_L \qquad (13)$$

where M_L is the mass per unit chain length. By substituting L_r with eq 13, eq 12 gives

$$[\eta] = 10^{-2}\Phi(L_r,d_r)M^{1/2}/(\lambda M_L)^{3/2} \qquad (14)$$

where Φ, the Flory viscosity constant, is a function of L_r and the reduced hydrodynamic diameter, d_r. The latter is related to the hydrodynamic diameter, d, by

$$d_r = \lambda d$$

Tables for $\Phi(L_r,d_r)$ were presented in ref 16.

By use of the table for Φ in ref 16 and eq 14, the values for q, d_r, and M_L were chosen by successive approximations to obtain the best fit for the intrinsic viscosity. The parameters thus estimated according to eq 14 are listed in Table V for PVI and QPVI in methanol/TBABr.

Table V
Parameters for the Wormlike-Chain Model

polymer	solvent	q, Å	M_L, g/Å	d_r	C_∞ (±10%)
PVI	MeOH/0.01 M TBABr	22–23	41	0.15	15
QPVI	MeOH/0.01 M TBABr	20	88	0.32	18

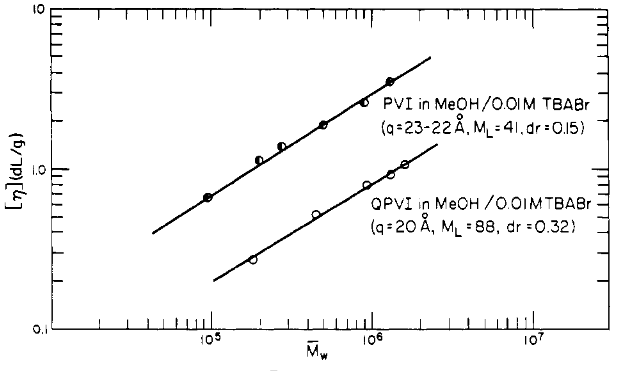

Figure 11. log $[\eta]$ vs. log $\bar{M}_w$ for PVI and QPVI in methanol/TBABr.

The relatively small numbers for q of the present polymers (i.e., 22–23 Å for PVI and 20 Å for QPVI), compared with those for semirigid rodlike macromolecules, such as DNA (q = 550 Å)[16] and poly(n-hexyl isocyanate) (q = 395–425 Å),[17] indicate the flexible and coillike nature of PVI and QPVI.

The Yamakawa–Fujii theory was formulated without taking into account the excluded volume effects. Thus the derived values for q and d_r discussed here should be taken as "apparent" values. These parameters are affected by the nature of the solvents in which the intrinsic viscosities were measured. For example, the $[\eta]$ value for PVI with $\bar{M}_w = 10^6$ (i.e., $[\eta]$ = 2.9 dL/g as shown in Figure 11) is higher than the value for QPVI with an equivalent number of monomer units (i.e., $[\eta]$ = 1.35 dL/g for $\bar{M}_w = [M_0(\text{QPVI})/M_0(\text{PVI})] \times 10^6 = 2.34 \times 10^6$; see Figure 11). These data suggest that MeOH is a better solvent for PVI than for QPVI with an identical number of monomer units. Thus, the smaller q value estimated for QPVI (q = 20 Å) compared with the value for PVI (q = 22–23 Å) should also reflect this difference in solvent power.

At first glance, the values for q as described above may lead one to conclude that QPVI is a slightly more flexible chain than PVI. This is true only in the solvent discussed (MeOH/0.01 M TBABr). On the contrary, the characteristic ratios in the absence of the excluded volume effect for the two polymers [C_∞(PVI) = 15 and C_∞(QPVI) = 18; Table IV or V] suggest that the PVI chain is more flexible than QPVI in the unperturbed state. Thus, the opposite trend in the orders for q and C_∞ for the two polymers is not contradictory but consistent with the fact that the two quantities were defined in different states.

Calculations of q based on light scattering data were not made here because of the lack of data on the polydispersity of the fractions.

Conclusions

Chain dimensions for the neutral polymer PVI are insensitive to the presence of neutral salts, whereas those for the charged polymers QPVI and HPVI are very sensitive to the nature and ionic strength of the added salts.

The order of the strength of counterion binding to these polycations was similar to the order for the Hofmeister series, acetate being the weakest and SCN⁻ being the strongest binding ions.

The unperturbed dimensions of the vinylimidazole-containing polymers vary only slightly with the nature of solvent or quaternary side group on the imidazole site but vary greatly with the counterion. The characteristic ratio is the largest ($C_\infty = 28$) when acetate or propionate is the counterion. In the presence of a stronger binding counterion, such as chloride, the characteristic ratio decreases to 15-18.

Both viscosity and light scattering data suggest that these polymers are coillike in methanol or aqueous salt solutions. The persistence lengths, calculated on the basis of the wormlike-chain model using the Yamakawa-Fujii scheme, are q = 22-23 Å for PVI and q = 20 Å for QPVI in methanol/0.01 M TBABr.

Acknowledgment. We thank Dr. H. Yu for his continuing interest in our work. We are grateful to Mr. W. A. Bowman and Dr. H. Cohen for the syntheses of the polymers.

References and Notes

(1) Gregor, H. P.; Gold, D. H. *J. Phys. Chem.* **1957**, *61*, 1347.
(2) Gold, D. H.; Gregor, H. P. *Z. Phys. Chem.* (*Frankfurt am Main*) **1958**, *15*, 93.
(3) Liu, K. J.; Gregor, H. P. *J. Phys. Chem.* **1965**, *69*, 1248.
(4) Overberger, C. G.; Smith, T. W.; Dixon, K. W. *J. Polym. Sci., Polym. Symp.* **1970**, *No. 50*, 1.
(5) Gold, D. H.; Gregor, H. P. *J. Phys. Chem.* **1960**, *64*, 1464.
(6) Henrichs, P. M.; Whitlock, L. R.; Sochor, A. R.; Tan, J. S. *Macromolecules* **1980**, *13*, 1375.
(7) Tan, J. S.; Gasper, S. P. *J. Polym. Sci., Polym. Phys. Ed.* **1975**, *13*, 1705.
(8) Tricot, M.; Mertens, G.; Collette, P.; Desreux, V. *Bull. Soc. R. Sci. Liege* **1974**, *43*, 502.
(9) Eskin, V. E.; Magarik, S. Ya.; Zhuruev, U. B.; Rudkovskaya, G. D. *Vysokomol. Soedin., Ser. A* **1978**, *20* (10), 2219.
(10) von Hippel, P. H.; Schleich, T. *Acc. Chem. Res.* **1969**, *2* (9), 257.
(11) Kratky, O.; Porod, G. *Recl. Trav. Chim. Pays-Bas* **1949**, *68*, 1106.
(12) Benoit, H.; Doty, P. *J. Phys. Chem.* **1953**, *57*, 958.
(13) Tanford, C. "Physical Chemistry of Macromolecules"; Wiley: New York, 1967; p 220.
(14) Krigbaum, W. R.; Flory, P. J. *J. Am. Chem. Soc.* **1953**, *75*, 1775.
(15) Krigbaum, W. R. *J. Am. Chem. Soc.* **1954**, *76*, 3758.
(16) Yamakawa, H.; Fujii, M. *Macromolecules* **1974**, *7*, 128.
(17) Rubingh, D. N.; Yu, H. *Macromolecules* **1976**, *9*, 681.

Symmetry Criteria in the Theory of Chain Polymer Hydrodynamics[†]

Marshall Fixman

Department of Chemistry, Colorado State University, Fort Collins, Colorado 80523.
Received April 13, 1981

ABSTRACT: The assumption that the motion of flexible-chain polymers can be modeled as that of a rigid body in certain stationary flows is examined. An explicit formula is derived for the center-of-mass velocity in sedimentary flow, based on several assumptions in the literature: (1) rigid-body motion, (2) coincidence of the axis of rotation with the direction of flow, and (3) isotropy of the unperturbed solution. An examination of the velocity formula shows that it fails to satisfy necessary symmetry requirements except in the special case where the angular velocity vanishes for all conformations. Since this condition on angular velocity will not be met unless hydrodynamic interaction is preaveraged, the set of assumptions is concluded to be generally inconsistent with the equations of diffusive motion for chain or other polymers. Quantitative estimates of the error are reached in an accompanying paper on the dynamical simulation of chains with hydrodynamic interaction.

I. Introduction

The assumption that flexible-chain polymers move as rigid bodies in sedimentary or simple shear flow has a long history. This examination of the hypothesis was stimulated by the recent work of Zimm,[1] who used the hypothesis to derived algorithms for the Monte Carlo calculation of the sedimentation constant and intrinsic viscosity of chain polymers. The purpose of his work was to eliminate the approximation of preaveraged hydrodynamic interaction (HI) in the calculation of these transport coefficients. Unfortunately, the hypothesis of rigid-body motion is here found to be inexact for flexible chains with fluctuating HI; with preaveraged HI the hypothesis is correct. This work can supply no estimates of the error that results from the hypothesis, but an accompanying dynamical simulation[2] indicates significant errors for sedimentary flow.

Our work is based on the diffusion equation for chain polymer motion and is unrestricted in the choice of chain potential. Any conventional HI is also allowed. We do assume that the HI interaction tensor is a function of chain coordinates and not of time. Thus solvent inertia as well as chain inertia is suppressed. Our intention has been to follow the assumptions used by Zimm, to obtain an explicit formula rather than an algorithm for the sedimentation constant, and to strengthen the appeal to symmetry. Examination of the explicit formula shows the contradictions inherent in the rigid-body hypothesis or, more precisely, in one particular form of that hypothesis: that the axis of rigid-body rotation coincides with the symmetry axis of the external force. This assumption is found to be defective even for truly rigid bodies.

The proper formulas for the sedimentation constant and intrinsic viscosity of a bead model without HI go back at least as far as Kramers.[3] Inclusion of HI makes for considerable difficulty. If the HI is preaveraged, formulas correct for any chain potential are available. For the in-

---

[†] Supported in part by NIH GM27945.